

# Shrouded wind turbine performance in yawed turbulent flow conditions

Wind Engineering  
XX(X):1–7  
©The Author(s) 2021  
Reprints and permission:  
sagepub.co.uk/journalsPermissions.nav  
DOI: 10.1177/ToBeAssigned  
www.sagepub.com/

SAGE

Gustavo Richmond-Navarro<sup>1</sup>, Takanori Uchida<sup>2</sup> and Williams R. Calderón-Muñoz<sup>3, 4</sup>

## Abstract

Wind turbines represent a growing energy source worldwide. In many cases, operating in turbulent and changing wind direction spots. In this work, we use a wind tunnel to analyse the effect of the turbulence in a wind turbine provided with a Wind Lens flow concentrator, under yaw conditions, for turbulence intensity values of 10% and 15%. Measurements are made of the power coefficient as a function of the Tip Speed Ratio using two types of Wind Lens, CiiB5 and CiiB10, at yaw angles from 0° to 30°. In general, for the turbine with Wind Lens, an increase of the yaw angle causes a reduction of the power coefficient. If the turbine operates with the CiiB10, the stronger the turbulence, the greater performance is obtained. In conclusion, for the case of turbulent flow and yaw = 20° or less, the Wind Lens turbine offers better performance than without the flow concentrator.

## Keywords

Yaw angle, Wind Lens, turbulence intensity, power coefficient

## Introduction

In view of the global energy needs, wind energy has become one of the main clean and cost-competitive energy sources worldwide. In 2019, 60.4 GW wind power were installed around the world, making a cumulative total of 651 GW GWEC (2019). Within this field, small-scale wind turbines also have grown. As a reference, a cumulative total of 990 000 small-scale wind turbines were installed in the world by the end of 2015 Pitteloud and Gsänger (2017). Small-scale wind turbines are commonly located at low heights, where there are wind speed fluctuations Tummala et al. (2016).

In the case of turbulent flow, flow concentrators have been studied in research literature as an alternative to improve performance. For example, in Kosasih and Hudin (2016) performance of a small-scale wind turbine equipped with a diffuser, under turbulent flow, is evaluated both experimentally in a wind tunnel and by means of Computational Fluid Dynamics (CFD); the conclusion is that diffusers improve performance quantitatively. On the other hand, Clements and Chowdhury (2019) also evaluates the performance of a turbine with a diffuser in turbulent flow at relatively slow speeds, specifically using the Wind Lens diffuser, and obtaining also an improvement in performance if using the flow concentrator. The Wind Lens has the benefit of increasing the output power Heikal et al. (2018), reducing noise Ohya et al. (2017a), improving safety Khamlaj and Rumpfkeil (2018) and being friendlier to birds than conventional turbines Hu and Wang (2015). Added to this, control of the turbine orientation is given by the Wind Lens ring itself Ohya and Karasudani (2010).

As Tummala et al. (2016) indicates, studies concerning the subject of wind speed fluctuation should be highly detailed in order to correctly describe actual wind conditions and their effect on the performance of wind turbines. As Pagnini et al. (2015) report, vertical and horizontal axis turbines are

negatively sensitive to turbulence, therefore placing them in complex topographies where turbulence is usually high should be avoided; Lubitz (2014) indicates that at low wind speed an increase in turbulence produces an increment in energy production. According to Wang et al. (2014), the lift force of the blades can increase with increasing turbulence and in Chu and Chiang (2014), experimental results found that power production with flows produced by grid-generated turbulence is slightly higher than with flows without turbulence.

A frequent condition under turbulent flow is misalignment of the turbine axis according to the direction of the incidental wind, which creates yaw angles different from zero. Studies on turbulent flow under yaw conditions, for turbulence intensities (TI) lower than 9% in a hydrokinetic turbine report minimum affectation in the power coefficient (Cp) Tian et al. (2016), in contrast with reports from Pagnini et al. (2015), who asserts that turbulence plays a crucial role in turbine efficiency; what is more, Rogers and Omer (2013) indicate losses of up to 20% of the power due to turbulent flow conditions. In the case of turbines with a flow concentrator, Rivarolo et al. (2020) report that there is an optimum yaw angle at which energy production is augmented, which is in function of the specific type of concentrator, contrasting with

<sup>1</sup> Department of Electromechanical Engineering, Instituto Tecnológico de Costa Rica, Costa Rica.

<sup>2</sup> Research Institute for Applied Mechanics (RIAM), Kyushu University, Fukuoka, Japan.

<sup>3</sup> Department of Mechanical Engineering, Faculty of Physical and Mathematical Sciences, Universidad de Chile, Santiago, Chile.

<sup>4</sup> Energy Center, Universidad de Chile, Santiago, Chile.

## Corresponding author:

Gustavo Richmond-Navarro, Department of Electromechanical Engineering, Instituto Tecnológico de Costa Rica, Costa Rica.

Email: grichmond@tec.ac.cr

the power reduction experimented by a conventional turbine under yaw conditions [Li et al. \(2016b\)](#), in which the yaw angle is minimized to maximize wind energy capture [Jing et al. \(2020\)](#), since average annual loss may reach up to 13% for an average yaw angle of  $15^\circ$  [Wan et al. \(2015\)](#).

Research conducted by [Li et al. \(2016b\)](#) presents the results of the power coefficient for yaw angles of  $0^\circ$ ,  $10^\circ$ ,  $20^\circ$  and  $30^\circ$ , for TI of 1.4%, 8% and 13.5% with a Reynolds number,  $Re = 1.3 \times 10^5$ . With angles  $0^\circ$ ,  $10^\circ$  and  $20^\circ$ , the power coefficient increases from TI = 1.4% to TI = 8%, and then decreases for TI = 13.5%. In the case of yaw =  $30^\circ$  the power decreases with increasing TI. On the other hand, [Li et al. \(2016a\)](#) studied the effect on performance of a wind turbine for flows with TI of 0.5% and 10%, under yaw conditions of  $0^\circ$  and  $30^\circ$  with  $Re = 1.5$  and  $2 \times 10^5$ . In this case, the power coefficient increases significantly for TI = 10%; in addition, for yaw =  $30^\circ$ , the power coefficients show values higher than under no-yaw condition.

As regards studies exclusively numerical, [Dighe et al. \(2019\)](#) confirm that ducted wind turbines exhibit superior performance than conventional turbines and demonstrate that a specific type of conventional turbine can be optimized. Meanwhile, [Dighe et al. \(2020\)](#) study the aerodynamic and acoustic performance of ducted wind turbines in yawed conditions, finding that for an angle of  $7.5^\circ$  the yaw effect is minimal in terms of power while noticeable regarding noise increase.

Although all results presented are obtained for different Reynolds numbers, with rotors provided of blades with varying aerodynamic profiles and pitch angles, yaw, turbulence intensity and the presence of a concentrator affect the efficiency of wind turbines, their effect depending on the way these parameters are combined. What is new in this paper is that it focuses on the simultaneous combination of the three factors, showing the performance of a wind turbine with two different flow concentrators of the type Wind Lens, in turbulent flow with TI of 10% and 15% under yaw conditions for angles of  $0^\circ$ ,  $10^\circ$ ,  $20^\circ$  and  $30^\circ$ .

## Materials and methods

### Equipment

The experiment was conducted in the boundary-layer wind tunnel at the Research Institute for Applied Mechanics (RIAM) of Kyushu University in Japan. The testing section is 15 m long, 3.6 m wide and 2 m high. The tests were carried out without the lateral and upper panels of sections 3, 4 and 5 indicated in Figure 1. Side panel 3 opposite to the fans was removed only partially. These considerations were taken to minimize the blocking effect [Ohya \(2019\)](#). Additional technical details of the wind tunnel can be found in [Ohya et al. \(2017b\)](#).

Turbulence was produced by means of a wooden grid placed in the structural frame between panels 2 and 3 of the testing section. Its dimensions are  $M = 156.2$  mm,  $b = 43.5$  mm and  $t = 29.9$  mm, see Figure 2.

The rotor used is shown in Figure 3, it has 3 blades, a diameter of 1 m and a pitch angle of  $4^\circ$ . The blades consists of three aerodynamic MEL type profiles, developed by [Matsumiya et al. \(2000\)](#), blended with different chord and

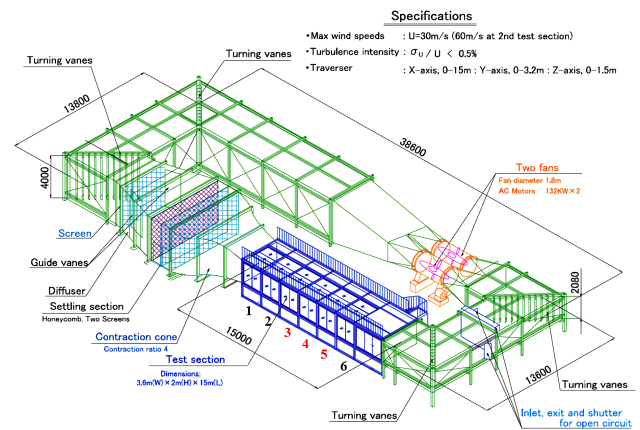


**Figure 1.** Boundary-layer wind tunnel, Kyushu University [Ohya et al. \(2017b\)](#).

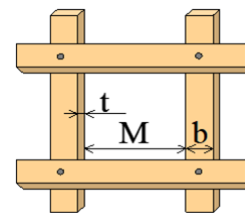


**Figure 2.** Dimensions of the turbulence grid.

**Table 1.** Aerodynamic profiles along the blade span.

Profile	Radial station (mm)	Twist ( $^\circ$ )	Chord (mm)
Root	76	59	73
MEL20	236	30	105
MEL18	378	14	74
MEL12	500	9	67



**Figure 3.** Wind turbine's rotor.

twist angles, as shown in Figure 4, with the specific values given in the Table 1.

The turbine was utilized with two types of Wind Lens, CiiB5 and CiiB10, whose characteristics are shown in Figure 5 and Table 2. The difference between both Wind Lens is the rear ring ( $h$  in Figure 5), which in case of CiiB5 is 50 mm high and its area is 23% of the free inside area of the rotor plane; for CiiB10 the ring height is 100 mm and its area is 48% of the free inside area in the rotor plane. Those

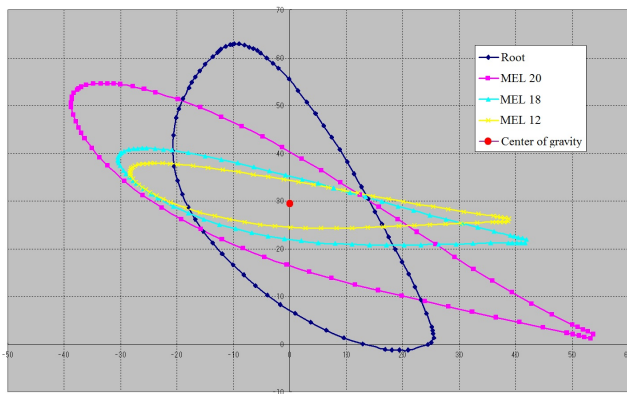


**Figure 4.** MEL profiles twist and chord distribution in the blades (dimensions in mm).

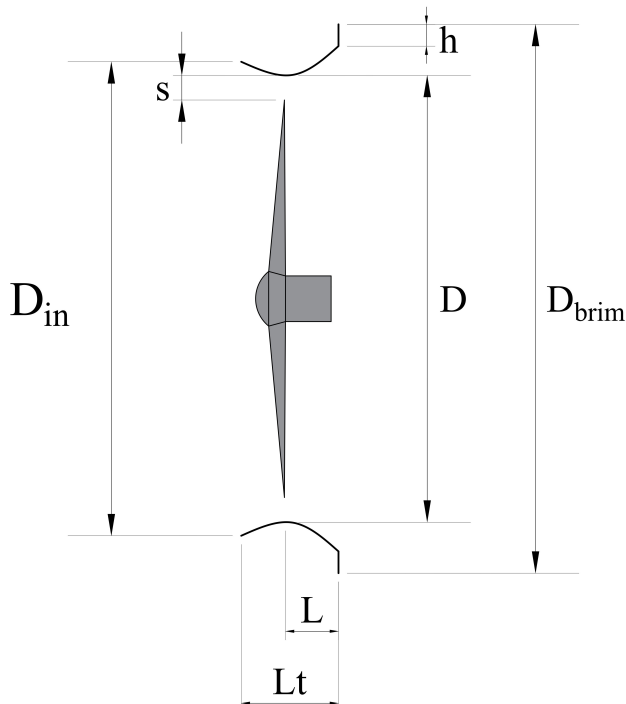


**Figure 5.** Wind Lens geometric parameters.

**Table 2.** Values of Wind Lens geometric parameters.

Parameter (mm)	CiiB5	CiiB5
$D_{brim}$	1263	1363
$D_{in}$	1080	1080
$D$	1030	1030
$L_t$	224	224
$L$	107	107
$h$	50	100
$s$	15	15

Wind Lens have been used by [Ohya and Karasudani \(2010\)](#) and [Richmond-Navarro et al. \(2021\)](#).

Wind speed was recorded with a hot wire anemometer model 0251R-T5 provided with a 5 micron diameter tungsten filament [KANOMAX \(2020\)](#). Each measurement point was evaluated during 30 s, with a sampling rate of 1 kHz and a low pass filter of 100 Hz. Turbulence intensity was calculated as the standard deviation of the wind measurements divided between the average [Burton et al. \(2011\)](#), during the same

**Table 3.** Experimental variables and levels.

Variable	Levels			
Turbulence intensity (%)	15	10		
Wind Lens	None	CiiB5	CiiB10	
Yaw angle (°)	0	10	20	30



**Figure 6.** Experimental set-up: the wind turbine with Wind Lens and turbulence grid.

30 s. The turbine was driven by a servomotor, which allows to govern its speed of rotation. A three-component force transducer with a maximum capacity of 15  $kg_f m$  was placed at the base of the servomotor to measure torque. The power was calculated by multiplying the rotor's torque ( $T$ ) by its angular speed ( $w$ ). The power coefficients were computed as the ratio of measured power by the maximum power available in the wind, as shown in equation 1.

$$C_p = \frac{T\omega}{\frac{1}{2}\rho v^3 \pi r^2}, \quad (1)$$

where  $\rho$  is the air density,  $v$  is the wind speed and  $r$  is the rotor radius, unless otherwise stated.

All equipment is connected to a data acquisition equipment that processes the signals and delivers the results in a Microsoft Excel table.

## Methodology

The experiment consists of measuring the power coefficient in function of the Tip Speed Ratio (TSR) for 24 possible combinations according to the variables and levels indicated in Table 3. The experiment was conducted with the turbulence grid in place at all times. In all cases the Reynolds number was of  $5.6 \times 10^5$ , computed by multiplying the rotor diameter by the free stream wind speed and divided by the kinematic viscosity of the air.

A speed correction is applied considering the blocking effect [Barlow et al. \(1999\)](#) and taking as a reference measurements made with a 3-axis ultrasonic anemometer installed in the tunnel in a fixed position, at the right of Figure 6. The experimental set-up of the turbine at a yaw angle, the Wind Lens in place and the turbulence grid used in the experiment can also be seen in Figure 6.

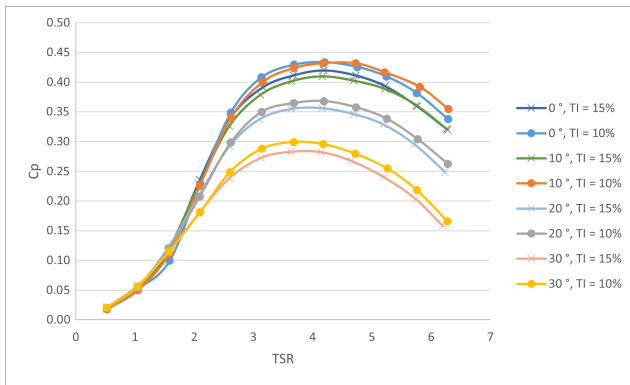


**Figure 7.** Turbine performance without Wind Lens, at yaw angles  $0^\circ$ ,  $10^\circ$ ,  $20^\circ$  and  $30^\circ$  and  $TI = 10\%$  and  $15\%$ .

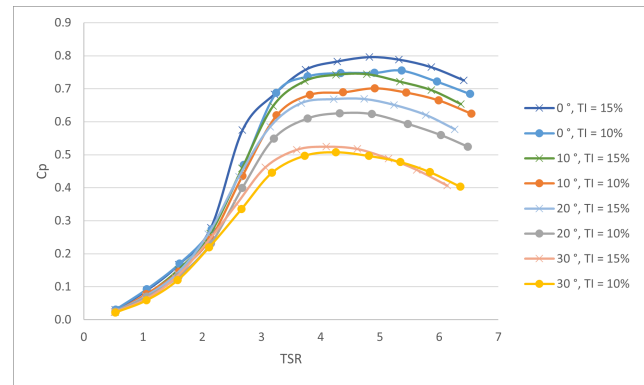


**Figure 8.** Turbine performance with the Wind Lens CiiB5, at yaw angles  $0^\circ$ ,  $10^\circ$ ,  $20^\circ$  and  $30^\circ$  and  $TI = 10\%$  and  $15\%$ .

## Results

By combining the two turbulence levels with the four yaw angles in Table 3, the performance of the turbine without Wind Lens, with CiiB5 and CiiB10 is shown in Figures 7, 8 and 9 respectively.

In the case of Figure 7 turbulence affects negatively turbine performance in all cases, with or without yaw angle. Between  $TSR = 4$  and  $4.5$  the turbine offers the maximum power coefficient, for both  $TI$  and at all yaw angles. Additionally, with increasing yaw angle the performance decreases, save for yaw =  $10^\circ$ . This situation of maximum power at non-zero yaw for a bare rotor under turbulent flow conditions, can be found in previous literature [Li et al. \(2016a\)](#), which stated that increasing the  $TI$  may increase the  $C_p$  considering that turbulence transition of the boundary layer could suppress the flow separation at the leading edge. In that research there was a low  $Re = 2 \times 10^5$  close to the value of  $Re = 5.6 \times 10^5$  of the present results.

Moreover, [Li et al. \(2016a\)](#) mention that  $TI$  can cause variations of the blade angle of attack during the rotation, and in yaw conditions the angle of attack has a periodic variation during the rotation. Hence, both  $TI$  and yaw conditions modify the angle of attack and may improve the performance at low  $Re$ . On the other hand the yaw angle reduces the effective area of the rotor with respect to the flow, so they are two competing effects, one that tends to improve performance at low  $Re$  and another that decreases the effective area and therefore tends to decrease the usable flow.

For all the above, the maximum power occurs at non-zero yaw because with the lowest yaw the benefit exceeds the area reduction, since the area reduction due to having yaw is the ratio of the area of an ellipse (the projection of the rotor area in the flow) on the rotor area that is circular. Since the vertical axis remains invariant, the reduction in area is proportional to the cosine of the yaw angle. For  $10^\circ$  the area is 98.48% of the original area but for  $20^\circ$  the area is 93.97% of the original area. Since the area reduction is non-linear and increases steeply at higher yaw angles, this improvement is obtained only for  $10^\circ$  for this particular rotor and Reynolds number from this study.

As illustrated in Figure 8 the maximum power coefficient is in the  $TSR$  closest to 5. This sliding of optimum  $TSR$  is usual in Wind Lens turbines. Now the power coefficient

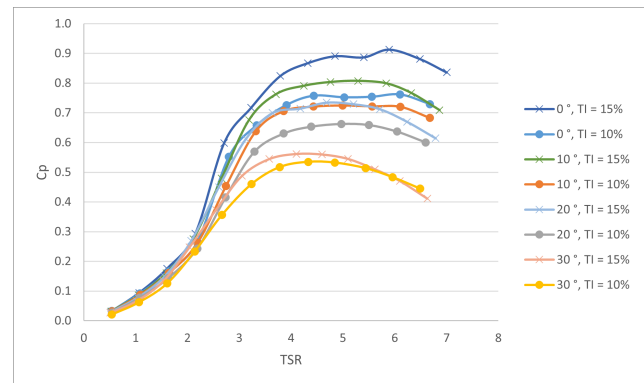


**Figure 9.** Turbine performance with the Wind Lens CiiB10, at yaw angles  $0^\circ$ ,  $10^\circ$ ,  $20^\circ$  and  $30^\circ$  and  $TI = 10\%$  and  $15\%$ .

is higher in case of  $TI$  of 15%, except for yaw  $30^\circ$ , where both curves are very similar. A decrease in performance with increasing yaw angle is also observed. Exceptions to this trend are not evident, as occurs with the turbine without flow concentrator.

Figure 7 illustrates the highest power coefficient recorded in the experiment. As with the CiiB5, the turbine equipped with the Wind Lens CiiB10 shows an increase in the value of the power coefficient with increasing turbulence. This effect is not recorded at a yaw angle of  $30^\circ$ . On the other hand, as the Wind Lens considerably increases the power coefficient compared to the turbine without flow concentrator, the results of Figures 7 to 9 indicate that in turbulent flow a turbine at yaw =  $20^\circ$  or less produces greater power than the bare turbine under no yaw conditions. Figure 10 illustrates the results obtained from calculating the percentage of variation of the power coefficient of the turbine operating without Wind Lens, with yaw angles of  $10^\circ$ ,  $20^\circ$  and  $30^\circ$ , for  $TI = 10\%$  and  $15\%$ . Notably, from  $TSR = 2$ , the curves for each yaw angle are very similar, with a very small difference where  $TI = 10\%$ , mainly for yaw =  $10^\circ$ . These results agree with reports from [Li et al. \(2016b\)](#) and [Li et al. \(2016a\)](#) where the power coefficient increases for  $TI = 8\%$  and  $10\%$  respectively. However, only for yaw =  $10^\circ$  the power coefficient is greater than for yaw =  $0^\circ$ , contrasting with results obtained by [Li et al. \(2016a\)](#) who report that it is at yaw =  $30^\circ$  where higher power coefficient values than at yaw =  $0^\circ$  occur. Aerodynamic profiles are different in the quoted references from those in the present research, which is to be

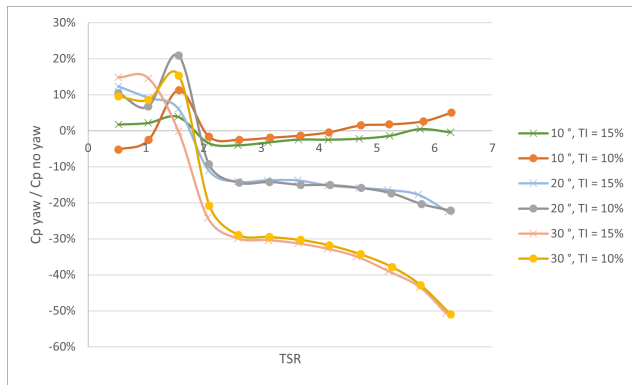


**Figure 10.** Increase or decrease percentage of Cp without Wind Lens with respect to no yaw at yaw angles  $10^\circ$ ,  $20^\circ$  and  $30^\circ$  and TI = 10% and 15%.

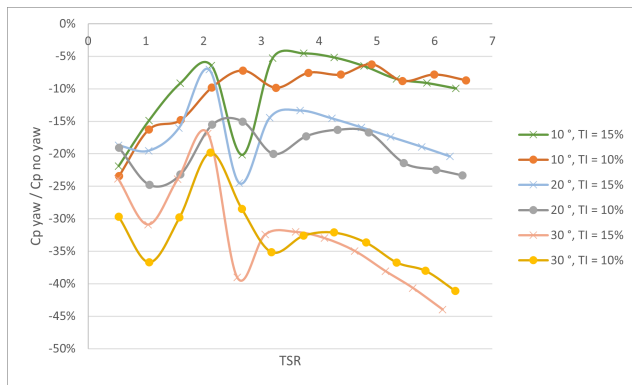


**Figure 11.** Percentage of Cp decrease with the Wind Lens CiiB5 with respect to no yaw, at yaw angles  $10^\circ$ ,  $20^\circ$  and  $30^\circ$  and TI = 10% and 15%.

taken into account. In general, an increase in the yaw angle leads to a decrease in the power coefficient because the area perpendicular to the flow is reduced. This trend can be clearly observed in Figure 10.

The previous calculation is made for a turbine equipped with the CiiB5 to obtain the percentage of variation of the power coefficient of the turbine operating at yaw angles of  $10^\circ$ ,  $20^\circ$  and  $30^\circ$ , for TI = 10% and 15% (Figure 11). Here the pattern of lower power coefficient at higher yaw angle repeats, since for all combinations, the power coefficients are lower than in the case of no yaw. There is no clear trend differentiating the cases 10% or 15% TI.

Figure 12 demonstrates the results of the calculation of the percentage of variation of the power coefficient of the turbine working at yaw angles of  $10^\circ$ ,  $20^\circ$  and  $30^\circ$ , for TI = 10% and 15%, equipped with the CiiB10. The pattern of low power coefficient with greater yaw angle repeats, while for all combinations the power coefficient is lower than in the case of no yaw. The relative power coefficient for TI = 15% is lower than for TI = 10% at all yaw angles. A decrease around TSR = 3 occurs and later recover in all curves, similar to the case of TI = 15% with CiiB5.

The fact that the power coefficient always decreases with the Wind Lens installed under yaw condition may be due to shielding of the Wind Lens body on the rotor. This is because in the Wind Lens turbine at yaw different from zero the rotor has less area exposed to flow than a turbine without Wind

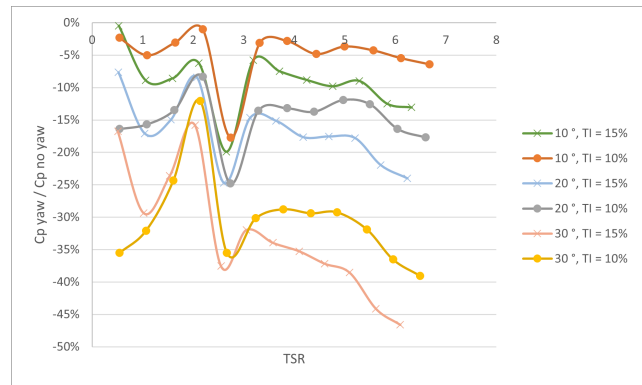


**Figure 12.** Percentage of Cp decrease with the Wind Lens CiiB5 with respect to no yaw, at yaw angles  $10^\circ$ ,  $20^\circ$  and  $30^\circ$  and TI = 10% and 15%.

Lens. Therefore, with turbulent flow the Wind Lens turbine's performance is more affected in percentage terms than one without Wind Lens.

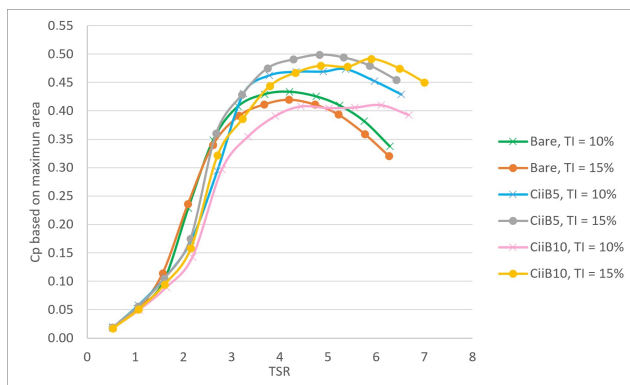
Finally, setting the yaw conditions aside, it is considered the question of whether a shrouded wind turbine exceeds the performance of a bare turbine if the comparison is based on maximum diffuser area. Up to this point, all power coefficients were computed using the rotor swept area, even in the cases where the Wind Lens was installed. Figure 13 shows the power coefficient for the two turbulence intensity levels at yaw angle  $0^\circ$ , but considering the external brim area in the Cp calculation for shrouded turbines (see Figure 5). These curves are the yaw =  $0^\circ$  cases in Figure 8, Figure 9 and Figure 10, but a reduction of 37.3% of Cp was made in the CiiB5 case and of 46.2% in the CiiB10 case as the brim areas are higher than the rotor swept area, according to data from Table 2.

Figure 13 shows that the turbine with the smaller Wind Lens exceeds the performance of a bare turbine with equivalent area but without exceeding the Betz limit. This supports the use of this type of technology and at the same time validates the results. When analyzing the case of the larger Wind Lens, it is observed that the performance decreases in this specific analysis of the Cp based on maximum diffuser area. This means that the flow concentration effect of the Wind Lens is not unlimited, that is, simply making it larger does not improve performance, since the increase in area is greater than increase in power captured when comparing the CiiB5 with the CiiB10 under the given conditions. Considering the big difference between the Cp curves for CiiB10 between both turbulence levels, these results suggest that for turbulent flow there could be an optimal size of Wind Lens as a function of the turbulence intensity, which is beyond the scope of this study.

## Conclusion

The analysis of the performance of the wind turbine operating under turbulent flow conditions, equipped with a Wind Lens flow concentrator under yaw condition led to the following conclusion:

For the turbine operating without Wind Lens, TI = 15% reduces the power coefficient compared to the one obtained with TI = 10%. This behavior is reversed in the case of the



**Figure 13.** Cp comparison based on maximum diffuser area without Wind Lens and with the Wind Lens CiiB5 and CiiB10, at yaw angle  $0^\circ$  and TI = 10% and 15%.

turbine equipped with the CiiB10, where the performance benefits from the increase in turbulence.

The turbine at yaw of  $20^\circ$  or less, but with Wind Lens, provides more power than a turbine without Wind Lens, in the case of turbulent flow.

The power coefficient under yaw conditions, relative to the power coefficient without yaw, is always lower with increasing yaw angle for the turbine operating with the Wind Lens.

The results of published literature were validated regarding the increase in the power coefficient in turbulent flow for bare wind turbines at yaw =  $10^\circ$ , after which value the power coefficient decreases.

A shrouded wind turbine can exceed the performance of a bare turbine even if the comparison is based on maximum diffuser area, but not for all geometries. Bigger diffuser may reduce the power coefficient.

### Declaration of conflicting interests

The authors declared no potential conflicts of interest with respect to the research, authorship, and/or publication of this article.

### ORCID iDs

Gustavo Richmond-Navarro <https://orcid.org/0000-0001-5147-5952>

Takanori Uchida <https://orcid.org/0000-0003-2630-9113>

Williams Calderón-Muñoz <https://orcid.org/0000-0003-3786-7495>

### Acknowledgements

We thank the Instituto Tecnológico de Costa Rica for financing this research and the Research Institute for Applied Mechanics (RIAM) of Kyushu University for providing the facilities for conducting the wind tunnel experiments. We also thank the technical staff who cooperated in conducting the tests at the Chikushi campus.

### References

- Barlow JB, Rae WH and Pope A (1999) *Low-speed wind tunnel testing, Third Edition*. John Wiley & sons.
- Burton T, Jenkins N, Sharpe D and Bossanyi E (2011) *Wind Energy Handbook, Second Edition*. John Wiley & Sons, Ltd.
- Chu CR and Chiang PH (2014) Turbulence effects on the wake flow and power production of a horizontal-axis wind turbine.

*Journal of Wind Engineering and Industrial Aerodynamics* 124: 82–89.

- Clements L and Chowdhury A (2019) Performance evaluation of wind lens in turbulent environment. *Energy Procedia* 160: 777–782.
- Dighe VV, Avallone F and van Bussel G (2020) Effects of yawed inflow on the aerodynamic and aeroacoustic performance of ducted wind turbines. *Journal of Wind Engineering and Industrial Aerodynamics* 201: 104174.
- Dighe VV, de Oliveira G, Avallone F and van Bussel GJ (2019) Characterization of aerodynamic performance of ducted wind turbines: A numerical study. *Wind Energy* 22(12): 1655–1666.
- GWEC (2019) Global wind report. Technical report, Global Wind Energy Council, Bruselas.
- Heikal HA, Abu-Elyazeed OS, Nawar MA, Attai YA and Mohamed MM (2018) On the actual power coefficient by theoretical developing of the diffuser flange of wind-lens turbine. *Renewable energy* 125: 295–305.
- Hu JF and Wang WX (2015) Upgrading a shrouded wind turbine with a self-adaptive flanged diffuser. *Energies* 8(6): 5319–5337.
- Jing B, Qian Z, Pei Y, Zhang L and Yang T (2020) Improving wind turbine efficiency through detection and calibration of yaw misalignment. *Renewable Energy* 160: 1217–1227.
- KANOMAX (2020) Hot-wire anemometer smart cta. URL <https://bit.ly/32XIu7c>.
- Khamlaj TA and Rumpfkeil MP (2018) Analysis and optimization of ducted wind turbines. *Energy* 162: 1234–1252.
- Kosasih B and Hudin HS (2016) Influence of inflow turbulence intensity on the performance of bare and diffuser-augmented micro wind turbine model. *Renewable Energy* 87: 154–167.
- Li Q, Kamada Y, Maeda T, Murata J, Yusuke N et al. (2016a) Effect of turbulence on power performance of a horizontal axis wind turbine in yawed and no-yawed flow conditions. *Energy* 109: 703–711.
- Li Q, Murata J, Endo M, Maeda T and Kamada Y (2016b) Experimental and numerical investigation of the effect of turbulent inflow on a horizontal axis wind turbine (part i: Power performance). *Energy* 113: 713–722.
- Lubitz WD (2014) Impact of ambient turbulence on performance of a small wind turbine. *Renewable Energy* 61: 69–73.
- Matsumiya H, Kogaki T, Takahashi N, Iida M and Waseda K (2000) Development and experimental verification of the new mel airofoil series for wind turbines. In: *Proceedings of Japan Wind Energy Symposium*, volume 22. pp. 92–95.
- Ohya Y (2019) Multi-rotor systems using five ducted wind turbines for power output increase (multi lens turbine). In: *AIAA Scitech 2019 Forum*. p. 1296.
- Ohya Y and Karasudani T (2010) A shrouded wind turbine generating high output power with wind-lens technology. *Energies* 3(4): 634–649.
- Ohya Y, Karasudani T, Nagai T and Watanabe K (2017a) Wind lens technology and its application to wind and water turbine and beyond. *Renewable Energy and Environmental Sustainability* 2: 2.
- Ohya Y, Miyazaki J, Göltenbott U and Watanabe K (2017b) Power augmentation of shrouded wind turbines in a multirotor system. *Journal of Energy Resources Technology* 139(5).

- Pagnini LC, Burlando M and Repetto MP (2015) Experimental power curve of small-size wind turbines in turbulent urban environment. *Applied Energy* 154: 112–121.
- Pitteloud JD and Gsänger S (2017) 2017 small wind world report summary. Technical report, World Wind Energy Association.
- Richmond-Navarro G, Casanova-Treto P and Hernández-Castro F (2021) Efecto de un difusor tipo wind lens en flujo turbulento. *Uniciencia* 35(2): 1–18.
- Rivarolo M, Freda A and Traverso A (2020) Test campaign and application of a small-scale ducted wind turbine with analysis of yaw angle influence. *Applied Energy* 279: 115850.
- Rogers T and Omer S (2013) Yaw analysis of a micro-scale horizontal-axis wind turbine operating in turbulent wind conditions. *International Journal of Low-Carbon Technologies* 8(1): 58–63.
- Tian W, VanZwieten JH, Pyakurel P and Li Y (2016) Influences of yaw angle and turbulence intensity on the performance of a 20 kw in-stream hydrokinetic turbine. *Energy* 111: 104–116.
- Tummala A, Velamati RK, Sinha DK, Indraj V and Krishna VH (2016) A review on small scale wind turbines. *Renewable and Sustainable Energy Reviews* 56: 1351–1371.
- Wan S, Cheng L and Sheng X (2015) Effects of yaw error on wind turbine running characteristics based on the equivalent wind speed model. *Energies* 8(7): 6286–6301.
- Wang S, Zhou Y, Alam MM and Yang H (2014) Turbulent intensity and reynolds number effects on an airfoil at low reynolds numbers. *Physics of Fluids* 26(11): 115107.